Vol. **111** (2007) *ACTA PHYSICA POLONICA A* No. 5

Proceedings of the XII National School "Correlated Electron Systems...", Ustroń 2006

Dynamical Mean Field within Iterative Perturbation Theory

B. Radzimirski and R.J. Wojciechowski

Institute of Physics, A. Mickiewicz University
Umultowska 85, 61-614 Poznań, Poland

We consider the iterative-perturbation theory and its generalization to multi-orbital Hubbard models. We discuss in detail all aspects of numerical implementations of the method.

PACS numbers: 71.10.–w, 71.10.Fd

1. Introduction

The problem of strong correlations belongs to the central problem of the condensed matter theory and has intensively been studied by many sophisticated methods. One of them is the dynamical mean field theory (DMFT) [1], which was successfully used to study, e.g. the metal–insulator (Mott) [2] transitions in strongly correlated electron systems. The simplest but nontrivial model that is used to study electron correlations is the Hubbard model, which in the limit of the infinite dimensions, is mapped onto a single impurity Anderson model. However, the Anderson-like models have to be solved together with appropriate self-consistent equations. In the limit of infinite dimension all spatial degrees of freedom are frozen and the self-energy is local (independent of momentum).

To solve the mapped single impurity model, one can adopt several computational schemes such as the quantum Monte Carlo method, the non-crossing approximation, the exact diagonalization method or iterative perturbation theory (IPT). The last scheme (i.e. IPT), introduced for the Hubbard model at half-filling [3, 4] and in [5] for arbitrary doping, allows us to solve the single impurity Anderson model in a very efficient and relatively simple way. The objective of this paper is to discuss the numerical implementations of IPT for orbitally degenerated models.

2. Model

We start with the following degenerate Hubbard-type model consisting of the noninteracting part H_0 and the exchange parts of the on-site Coulomb interaction H_1:

$$H_0 = \sum_{im\sigma i'm'\sigma'} \frac{h^{ii'}_{mm'\sigma}}{\sqrt{d}} c^{\dagger}_{im\sigma} c_{i'm'\sigma'} + \varepsilon^0_d \sum_{im\sigma} c^{\dagger}_{im\sigma} c_{im\sigma}, \tag{1}$$

$$H_1 = +\frac{1}{2} \sum_{im\sigma} U^i_{mm} n_{im\sigma} n_{im-\sigma} + \frac{1}{2} \sum_{im\neq m'\sigma} U^i_{mm'} n_{im\sigma} n_{im'-\sigma} + \frac{1}{2} \sum_{i\sigma m\neq m'} (U^i_{mm'} - J^i_{mm'}) n_{im\sigma} n_{im'\sigma}, \tag{2}$$

where ε^0_d and $h^{ii'}_{mm'\sigma}$ are the localized energy and hopping integral, respectively. The on-site interactions are described by three parameters U^i_{mm}, $U^i_{mm'}$, and $U^i_{mm'} - J^i_{mm'}$. The parameters U and J describe the on-site Coulomb repulsion and the exchange term which originates from the Hund coupling, respectively.

The hopping integral has to be rescaled in order to ensure that the density of states has a proper limit form. In the case of the nearest neighbors hopping the hopping integral is divided by the factor $\sqrt{2d}$. The chemical potential μ is determined to satisfy the Luttinger theorem. Moreover, the Hamiltonian (2) is rotationally invariant both in spin and real spaces. In addition to the local character of the self-energy coming from the Hubbard model in the limit of infinite dimensions, we assume that the self-energy as well as appropriate Green's functions G are diagonal with respect to the orbital index m. It means that there is no spontaneous symmetry breaking (i.e. all orbitals are equivalent). Thus, the self-energy and the local Green function take the forms [6]:

$$\Sigma_{ijmm'}(\omega) = \delta_{ij}\delta_{mm'}\Sigma(\omega),$$

$$G_{iimm'}(\omega) = \delta_{mm'}G(\omega).$$

For simplicity, we assume $U^i_{mm'} = U$ and $J^i_{mm'} = J$. The appropriate single impurity Anderson model has the following form:

$$H'_0 = \sum_{m\sigma} \varepsilon_{dm} d^{\dagger}_{m\sigma} d_{m\sigma} + \sum_{km\sigma m'\sigma'} \varepsilon_{km} c^{\dagger}_{km\sigma} c_{km'\sigma'} + \sum_{km\sigma} V_{km}(d^{\dagger}_{m\sigma} c_{km\sigma} + \text{h.c.}), \tag{3}$$

$$H'_1 = +\frac{1}{2} \sum_{m\sigma} U_{mm} n^d_{m\sigma} n^d_{m-\sigma} + \frac{1}{2} \sum_{m\neq m'\sigma} U_{mm'} n^d_{m\sigma} n^d_{m'-\sigma} + \frac{1}{2} \sum_{\sigma m\neq m'} (U_{mm'} - J_{mm'}) n^d_{m\sigma} n^d_{m'\sigma}, \tag{4}$$

where H_1' describes interaction at the impurity site. The initial Hubbard model is connected to the one impurity Anderson model by the following self-consistency condition:

$$\Delta(\omega) = h^2 G(\omega), \tag{5}$$

where the hybridization function $\Delta(\omega)$ is given by the conduction band energy levels ε_{km} and the corresponding hybridization matrix elements V_{km}:

$$\Delta(\omega) = \sum_{km} \frac{V_{km}^2}{\omega - \varepsilon_{km}}. \tag{6}$$

3. Iterative perturbation method

IPT was developed for an arbitrary doping and one-band Hubbard model in [5] whereas in [6] the method was generalized for a multi-orbital Hubbard model. Within the iterative perturbation approach the self-energy for small U is exact up to order U^2 and can be written in the form

$$\Sigma(\omega) = Un(N_{\mathrm{deg}} - 1) + \frac{A\Sigma^{(2)}(\omega)}{1 - B(\omega)\Sigma^{(2)}(\omega)}, \tag{7}$$

where N_{deg} is the total degeneracy and equals 2 (spin degeneracy). $\Sigma^{(2)}(\omega)$ is the second-order contribution of the self-energy. The parameter A is determined to fulfill the condition that the self-energy is exact in the limit of high frequencies and B is determined from the atomic limit. In addition, we can easily reproduce the case of vanishing interaction $U = 0$, of the completely filled and empty band.

Let us make a few remarks on validity of the IPT approach. As known, there is a difference in the width of the Kondo resonance between IPT and quantum Monte Carlo results. IPT is less accurate for very small doping, which results in overestimation of the Kondo energy scale. It is connected with a perturbative character of the IPT method. This method, as any perturbative method, cannot reproduce the exponentially small energy scale characteristic of Kondo-like behavior [7]. We should remember that IPT is a dynamical mean-field type of approximation, and therefore, it does not take into account spatial fluctuations (the self-energy is independent of the momentum), but includes the quantum dynamical fluctuations which are specially important for intermediate and strong correlations. One should be careful when the IPT method is adopted, because solutions of IPT depend on the initial value of the self-energy. And, if we start with the zero value of the self-energy we obtain a metallic solution for weak interaction, whereas for the self-energy proportional to U^2 we get an insulating solution for strong interaction. Moreover, IPT fails to converge close to metal–insulator critical point [8]. One more point concerning IPT is worthy of notice. Mainly, IPT takes into account exactly the moments of the spectral density up to the second. Modification of IPT [9] shows that also the third moment can be exactly calculated. This is especially important when a magnetic phase transition is considered. In this paper, however, we consider the metallic state only.

The self-energy in the limit $\omega \to \infty$ can be calculated from the condition

$$\lim_{\omega\to\infty} \omega\{\Sigma(\omega) + \langle\{[H'_I, d_{m\sigma}], d^\dagger_{m'\sigma}\}\rangle\}$$
$$= \langle\{[H'_I, d_{m\sigma}], [d^\dagger_{m'\sigma}, H_I]\}\rangle - \langle\{[H'_I, d_{m\sigma}], d^\dagger_{m'\sigma}\}\rangle^2. \tag{8}$$

To fix the parameter B we have calculated the appropriate Green function in the atomic limit for the degenerated model (see e.g. [6]). The final forms of the parameters A and B are

$$A = \frac{(x-a)(x-b)}{x\left[(a+b)^2 - ab - U^2\right] - (a+b)ab}, \tag{9}$$

$$B = \frac{\omega - \varepsilon_{dm} + \tilde{\mu}}{U^2(N_{\rm deg}-1)n_0(1-n_0)}, \tag{10}$$

where n_0 is the occupation number for the effective Anderson model determined together with the effective chemical potential $\tilde{\mu}$ which is connected with n_0 via the Luttinger theorem. n is the occupation number per each orbital and is defined by the relation

$$n_d = \sum_{m\sigma} n_{im\sigma} = nN_{\rm deg}.$$

The parameters a, b, and x are functions which depend on n_d, ω, and the parameters of the model.

IPT for non-degenerate case can be easily recovered when we put $N_{\rm deg} = 2$ ($n_d = 2n$).

3.1. Second-order contribution to the self-energy

Let us describe in detail the numerical procedure which we used to solve the DMFT self-consistent equations. The expression for the second-order contribution to the self-energy

$$\Sigma_0^{(2)}(\omega) := U^2 \int_{-\infty}^{0} {\rm d}\epsilon_1 \int_0^{\infty} {\rm d}\epsilon_2 {\rm d}\epsilon_3 \frac{\rho^{(0)}(\epsilon_1)\rho^{(0)}(\epsilon_2)\rho^{(0)}(\epsilon_3)}{\omega + \epsilon_1 - \epsilon_2 - \epsilon_3 - {\rm i}\eta}$$
$$+U^2 \int_0^{\infty} {\rm d}\epsilon_1 \int_{-\infty}^{0} {\rm d}\epsilon_2 {\rm d}\epsilon_3 \frac{\rho^{(0)}(\epsilon_1)\rho^{(0)}(\epsilon_2)\rho^{(0)}(\epsilon_3)}{\omega + \epsilon_1 - \epsilon_2 - \epsilon_3 - {\rm i}\eta} \tag{11}$$

can be factorized by replacing the denominator according to

$$\frac{1}{\omega + \epsilon_1 - \epsilon_2 - \epsilon_3 - {\rm i}\eta} = \frac{1}{z + \epsilon_1 - \epsilon_2 - \epsilon_3}$$
$$= {\rm i}\int_0^{\infty} {\rm d}\lambda \exp(-{\rm i}\lambda({\rm z} + \epsilon_1 - \epsilon_2 - \epsilon_3)) \tag{12}$$

($\eta > 0$). The self-energy can now be expressed in the form of the product of one-dimensional integrals. Those integrals take the form of the Laplace transforms

$$\tilde{\rho}_{\pm}(t) = \int_0^{\infty} \rho^0(\pm\omega){\rm e}^{{\rm i}\omega t}{\rm d}\omega, \tag{13}$$

where

$$\tilde{\sigma}_{\pm} = U^2 \tilde{\rho}_{+}(t)\tilde{\rho}_{-}(t)\tilde{\rho}_{\pm}(t). \tag{14}$$

Thus the expression for the second-order contribution takes the form

$$\Sigma_2(\omega - \mathrm{i}\eta) = \mathrm{i}\int_0^{\infty} [\tilde{\sigma}_{+}(\mathrm{t}) + \tilde{\sigma}_{-}(-\mathrm{t})]\mathrm{e}^{-\mathrm{i}\omega t}\mathrm{d}t. \tag{15}$$

This representation makes the numerical solution of the problem particularly fast and efficient. To calculate numerically the Laplace transforms we have used the continuous Fourier transform by padding the appropriate range by zeros. We have used the algorithm of the fast Fourier transform (FFT) to calculate discrete Fourier transform. From the latter one it is easy to obtain the continuous Fourier transform. The procedure allows us to calculate the self-energy in the self-consistent loop in a reasonable time. The integration in Eq. (13) can be reduced to an appropriate finite interval, since the density of states ρ^0 is exponentially localized as a function of frequency [10]. This is rather less obvious in the case of integration in Eq. (15), because the Laplace transforms (Eq. (14)) have long time tails of order $\mathrm{O}(t^{-3})$. However, it appears that the expression in square brackets in (15) is the Fourier transform of the smooth spectral function $\sigma(\omega)$ which is exponentially localized in time instead of having the long time tails. Therefore, the integration in Eq. (15) may also be reduced to appropriate finite time interval. Numerically, the Laplace transform is calculated by using the Fourier transform which can be done by padding the lower range, from the infinity to zero, by zeros. We approximate the continuous Fourier transform using algorithm for discrete Fourier transform. This can be done by approximation of the Fourier integral by a discrete sum

$$\int_{-\infty}^{\infty} h(t)\mathrm{e}^{2\pi \mathrm{i} f_n t}\mathrm{d}t \approx \sum_{k=0}^{N-1} h_k \mathrm{e}^{2\pi \mathrm{i} kn/N}\Delta = \Delta \sum_{k=0}^{N-1} h_k \mathrm{e}^{2\pi \mathrm{i} kn/N}. \tag{16}$$

The sum in Eq. (13) is calculated by the FFT algorithm used in [11]. In numerical application we have a function which is evenly sampled with some tiny fixed interval Δ. For such a value of Δ it is useful to define so-called the *Nyquist critical frequency* $f_{\mathrm{c}} \equiv 1/(2\Delta)$. This quantity plays an important role by two reasons. The first is when a continuous function, sampled at an interval Δ, is band width limited to frequencies smaller in magnitude than f_{c}, then the function is completely determined by a finished number of samples. This problem is known as a *sampling theorem*. The second is when we sample the continuous function which is not *band width* limited to less than the Nyquist critical frequency. We have an *aliasing* effect. In the latter, it turns out that all the values that lie outside of the frequency range $-f_{\mathrm{c}} < f < f_{\mathrm{c}}$ are spuriously moved into the range, which causes the numerical errors. To avoid errors connected with aliasing in our calculation we choose simply the small sampling interval of order $\Delta = 0.0005$. The above-described method allows us to calculate integrals with assumed degree of accuracy. In Figs. 1 and 2, respectively, we present the self-energy and density of states for several models parameters and doping as functions of the energy ω. These numerical calculations reproduce the results obtained in [10].

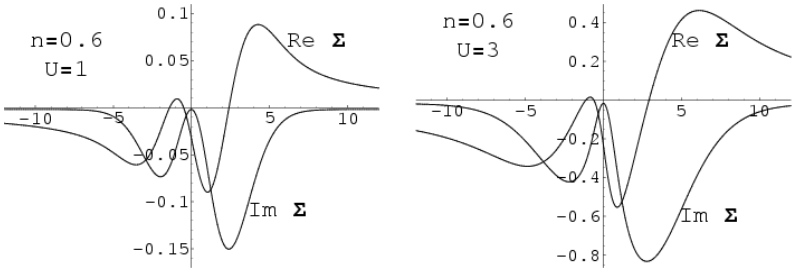

Fig. 1. Real and imaginary parts of the self-energy versus ω [eV] for $n = 0.6$ and $U = 1$ eV, $U = 3$ eV for the weak coupling scheme. The self-energy is calculated from Eq. (11).

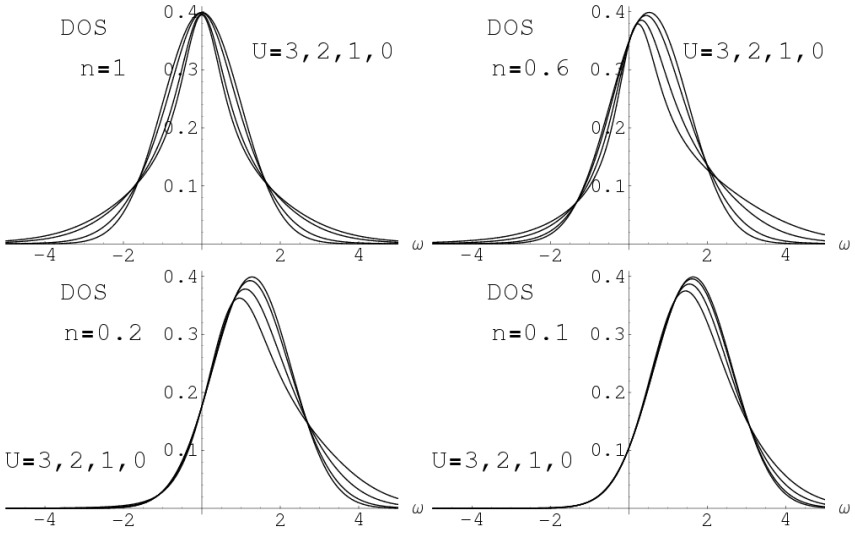

Fig. 2. Densities of states as a function of ω [eV] obtained in the weak-coupling theory for some values of filling (the result for half-filling is also included). U is given in eV.

3.2. Iterative perturbation loop

The idea of the iterative perturbation scheme with arbitrary filling is to construct a self-energy expression which retains features of arbitrary doping and reduces at half-filling to the ordinary IPT scheme. To retain the feature of half--filling we postulate the expression of the self-energy in the form given in Eq. (7). The second-order contribution to the self-energy is given by Eq. (11). The density of states $\rho^{(0)} = (1/\pi)\mathrm{Im}\, G_0$ calculated from the fictitious advanced Green function is given by

$$G_0(\omega) = \frac{1}{\omega + \mu_0 + \mu - \Sigma_{\mathrm{int}}(\omega)}. \tag{17}$$

The fictitious chemical potential μ_0 in (17) is given by $-\mu - Un$. It is easy to see that μ_0 vanishes at half-filling, giving the ordinary IPT scheme for the half-

-filling [5]. The full Green function takes the form

$$G_f(\omega) = \frac{1}{G_0^{-1} - \mu_0 + \mu - \Sigma_{\rm int}(\omega)}. \tag{18}$$

The interpolating form of the self-energy (11) is done to ensure the correctness of this approximation in different limits. The parameters A and B are given in Eqs. (9) and (10). The occupation numbers n and n_0 are calculated from $n_0 = \int_{-\infty}^{0} {\rm d}\omega {\rm Im}\, G_0(\omega)$ and $n = \int_{-\infty}^{0} {\rm d}\omega {\rm Im}\, G_f(\omega)$, respectively. Having the parameters A and B we have to modify the definition of the chemical potential μ_0. The parameter μ_0 is still free. Next, we fix μ_0 by imposing the Friedel sum rule (see for instance [5]) in the form

$$n = \frac{1}{2} - \frac{1}{\pi} \arctan\left(\frac{-\mu + \Sigma_{\rm int}(0) + {\rm Re}\Delta(0)}{{\rm Im}\,\Delta(0)}\right) + \int_{-{\rm i}\infty}^{{\rm i}\infty} \frac{{\rm d}\omega}{2\pi{\rm i}} G_f(\omega) \frac{\partial \Delta(\omega)}{\partial \omega}. \tag{19}$$

This is equivalent to the Luttinger theorem [12]: $\int_{-{\rm i}\infty}^{+{\rm i}\infty} ({\rm d}\omega/2\pi{\rm i}) G_f(\omega)(\partial \Sigma_{\rm int}(\omega)/\partial\omega) = 0$. In the case of the Hubbard model, the Luttinger theorem takes the simple form [10]:

$$\mu_0 = \mu - \Sigma_{\rm int}(\omega = 0), \qquad \mu_0 := \mu|_{U=0}. \tag{20}$$

The use of the Luttinger theorem is the main difference to earlier approximation schemes. It is essential to obtain a good agreement of IPT with the exact diagonalization method. The above-described method represents approximations between four good defined limits: strong and weak coupling, high and low frequency. To obtain the physical properties we can confine to calculation of G_f. We can do this by using the following iteration loop in which μ_0 is kept fixed:

a) At the beginning we guess the Green function G_f and the chemical potential μ.

b) Having the Green function, we calculate the hybridization $\Delta(\omega)$ from the formula

$$\Delta(\omega) = t^2 G_f(\omega), \tag{21}$$

which is the self-consistent condition in DMFT scheme for the Hubbard model in the infinity dimensions on the Bethe lattice.

c) At this stage we calculate the particle number $n = \int_{-\infty}^{0} {\rm d}\omega {\rm Im}\, G_f(\omega)$. When we are the first time in the loop μ_0 is calculated from

$$\mu_0 = \mu - Un. \tag{22}$$

Otherwise we calculate n from Eq. (22) which allows us to keep μ_0 fixed during calculations.

d) Having all previous quantities, we can calculate G_0 together with the fictitious density of states $\rho^{(0)} = (1/\pi){\rm Im}\, G_0$ and n_0

$$n_0 = \int_{-\infty}^{0} {\rm d}\omega G_0(\omega). \tag{23}$$

e) Next, the density of states $\rho^{(0)}$ is used to calculate the second-order contribution to the self-energy $\Sigma^{(2)}(\omega)$.

f) Having all quantities, necessary to determine parameters A and B, we determine the interpolating self-energy $\Sigma_{\rm int}(\omega)$.

g) From the Luttinger theorem we update the chemical potential μ

$$\mu = \mu_0 + \Sigma_{\rm int}(0). \tag{24}$$

New chemical potential is necessary to establish correct low energy behavior.

h) The new μ is used to calculate the Green function G_f (18) and we come to the beginning of the loop.

The iteration of the above procedure is continued until the convergence is attained. To compare results obtained from IPT with other methods, e.g. with the exact diagonalization it is convenient to use integrated spectral weight

$$F(\omega) := (1/\pi) \int_{-\infty}^{\omega} {\rm d}\tilde{\omega} {\rm Im}\, G_f(\tilde{\omega}). \tag{25}$$

The numerical results of the above method for the case of half-filling are presented in Fig. 3.

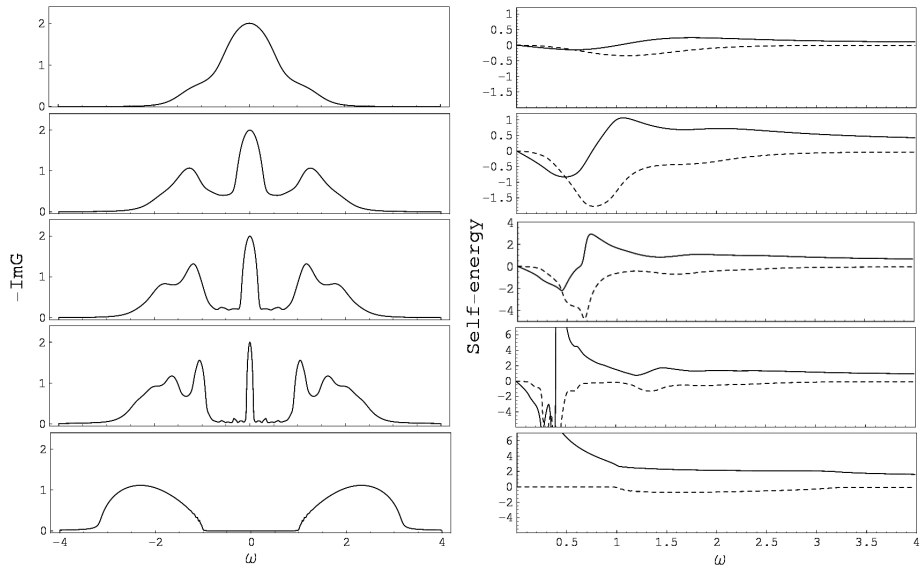

Fig. 3. Local spectral density ${\rm Im}\, G(\omega[{\rm eV}])$ (left figure) at $T = 0$, for several values of U, obtained by the IPT in the case of half-filling. The plots are drawn for the subsequent values of $(U[{\rm eV}] = 1, 2, 2.5, 3, 4)$ beginning from the top. The first four curves correspond to an increasingly correlated metal, the last graph presents an insulator [2]. Real (full line) and imaginary parts (dashed line) of the self-energy as functions of the real frequency $\Sigma(\omega + {\rm i}0^+)$ (right figure), for the same values of U as in the left figure. In the right figure graph at the bottom $(1/\omega)$ singularity in ${\rm Re}\Sigma$ can be seen.

4. Concluding remarks

The real advantage of the IPT scheme is a smooth density of states. Our scheme exhibits the feature of finite shift of the Kondo peak from the insulating band when the doping goes to zero. This is easily seen when we observe the dependence of density of states as a function of doping. This is the most striking feature of the Hubbard model, which did not appear both in earlier studies of this model in large dimensions using Monte Carlo techniques and in exact diagonalization algorithms.

Our preliminary calculations of the density of states give reasonable results at low temperatures which agree with those for the non-degenerate case [4, 5]. This is consistent with the general results obtained in [13] where it is shown that the nature of the Mott transition is not qualitatively changed by orbital degeneracy. The importance of degeneracy will be more evidenced if spontaneous symmetry breaking (e.g. non-paramagnetic phases) is taken into account.

Acknowledgments

A partial support from the Foundation for Polish Science (FNP) is gratefully acknowledged.

References

[1] A. Georges, G. Kotliar, W. Krauth, M. Rozenberg, *Rev. Mod. Phys.* **68**, 13 (1996).

[2] S. Florens, A. Georges, G. Kotliar, O. Parcoller, *Phys. Rev. B* **66**, 205102 (2002).

[3] A. Georges, G. Kotliar, *Phys. Rev. B* **45**, 6479 (1992).

[4] M. Jarell, *Phys. Rev. Lett.* **69**, 168 (1992).

[5] H. Kajueter, G. Kotliar, *Phys. Rev. Lett.* **77**, 131 (1996).

[6] T. Fujiwara, S. Yamamoto, Y. Ishii, *J. Phys. Soc. Jpn.* **72**, 777 (2003).

[7] Th. Prushke, R. Bulla, M. Jarell, *Phys. Rev. B* **61**, 12799 (2000).

[8] V. Janiš, *J. Phys., Condens. Matter* **10**, 2915 (1998).

[9] M. Pothoff, T. Wegner, W. Nolting, *Phys. Rev. B* **55**, 16132 (1997).

[10] E. Muller-Hartmann, *Z. Phys. B — Condensed Matter* **76**, 211 (1989).

[11] W.H. Press, B.P. Flannery, S.A. Teukolsky, W.T. Vetterling, *Numerical Recipes in FORTRAN: The Art of Scientific Computing*, 2nd ed., Cambridge University Press, Cambridge 1992, Ch. 12, p. 490.

[12] J.M. Luttinger, J.C. Ward, *Phys. Rev.* **118**, 1417 (1960).

[13] G. Kotliar, H. Kajueter, *Phys. Rev. B* **54**, 14221 (1996).